
Dynamic Beam Enumeration: A Bridge Between Generative Molecular Design and Library Screening

Anonymous Author(s)

Affiliation

Address

email

Abstract

1 Previous work reporting Beam Enumeration showed that *probable* substructures
2 extracted from a generative model contains chemically meaningful information
3 and can act as a source of explainability. In this work, we propose **Dynamic Beam**
4 **Enumeration** as an extension to extract *larger* substructures. We show that this
5 extracted insight can be made *actionable* and used to filter compounds in ultra-large
6 make-on-demand libraries (10^{9-12}). The resulting molecules possess properties
7 more aligned with the target objective than random sampling. Importantly, the
8 results suggest that Dynamic Beam Enumeration can act as a bridge between
9 generative design and library screening, such that even if generated molecules
10 cannot be easily synthesized, extracted knowledge from the model can be used to
11 find promising molecules that are make-on-demand.

12 1 Introduction

13 Molecular generative models have designed *experimentally validated* small molecule inhibitors¹
14 and catalysts². However, *synthesizability* remains a challenge as many generative approaches do
15 not explicitly enforce a notion of synthesizability. To this end, existing solutions include manual
16 prioritization by expert chemists, which is not scalable. Algorithmic solutions include synthesizability
17 heuristics based on historic data³⁻⁶ or synthesizability-constrained generation which enforces chemi-
18 cally feasible transformation during generation⁷⁻¹⁵. Alternatively, retrosynthesis models¹⁶⁻²⁸, which
19 predict feasible synthetic routes given a target molecule, can be included as an optimization objective
20 during molecular generation^{29,30} or for *post-hoc* filtering³¹. On the other side of the spectrum (Fig.
21 1b), virtual screening (VS), which aims to identify promising candidate molecules from *fixed* datasets
22 containing synthesizable molecules continues to be a productive approach to molecular discovery in
23 light of ultra-large molecular libraries (10^{9-12})³²⁻³⁷.

24 Previous work introduced Beam Enumeration³⁸ which extracts *probable* molecular substructures
25 during a language-based generative model’s optimization trajectory (towards the target objective).
26 These substructures were shown to be aligned with the target property profile. In this work, we
27 propose **Dynamic Beam Enumeration (DBE)** as an extension of Beam Enumeration to extract
28 probable *large* substructures from a model checkpoint. This contrasts Beam Enumeration which uses
29 extracted substructures only *during* optimization. These *large* substructures form a considerable part
30 of a full molecule and can be used to screen make-on-demand molecular libraries, such that molecules
31 with matching substructures are enriched in the properties of interest. These *initial* results suggest the
32 potential for DBE to act as a bridge between generative molecular design and VS, demonstrating
33 how extracted knowledge can be made *actionable*. Importantly, matched compounds are presumably
34 synthetically accessible, overcoming potential synthesizability challenges of *de novo* generated
35 molecules.

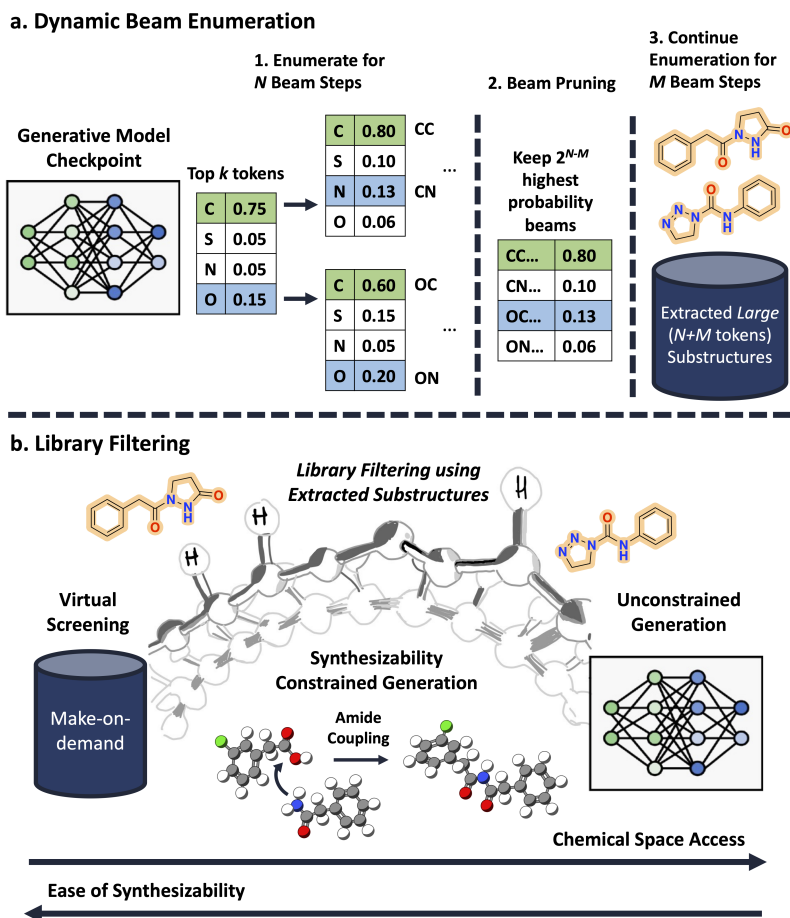


Figure 1: Dynamic Beam Enumeration. **a.** To enable the extraction of larger substructures, enumerated beams are pruned and only those with the highest probability are kept and further enumerated. **b.** Extracted large substructures can be used to filter make-on-demand libraries to *directly* identify promising molecules, acting as a bridge between generative design and screening.

36 2 Methods

37 **Dynamic Beam Enumeration.** We start from the Augmented Memory³⁹ language-based (LSTM⁴⁰
 38 RNN) molecular generative model which generates molecules as SMILES⁴¹. Previous work extended
 39 Augmented Memory with Beam Enumeration³⁸ which exhaustively enumerates the top k (2 in this
 40 work) tokens for N (18 in this work) beam steps, resulting in k^N token sub-sequences. These are
 41 *sub-sequences* which map to *substructures* because they are incomplete SMILES and do not map to a
 42 full molecule yet. The Beam Enumeration work showed that larger substructures are more meaningful
 43 and the maximum size that can be extracted is directly controlled by the number of beam steps. The
 44 authors stated that 18 beam steps is the limit (on a 24GB GPU) due to exponentially increasing
 45 memory requirements. In this work, we propose DBE to prune the sub-sequences set and enable the
 46 remaining beams to continue enumeration (Fig. 1a). Specifically, at the end of the N beam steps, we
 47 keep only the top (by probability) $N - M$ beams (M is 12 in this work), resulting in k^{N-M} beams
 48 left. These remaining beams are enumerated for M more steps, resulting in sub-sequences $N + M$
 49 tokens long, which map to larger substructures (Appendix A).

50 **Goal-directed Generative Design.** In this work, the use case of DBE is to extract large substructures
 51 from a model checkpoint and then use it to filter a make-on-demand library. Therefore, the first step
 52 is to task Augmented Memory³⁹ with optimizing a target objective. The case study is to generate
 53 molecules with good QuickVina2-GPU-2.1⁴²⁻⁴⁴ docking scores to ATP-dependent Clp protease
 54 proteolytic subunit (ClpP) which is implicated in cancer⁴⁵. The objective function is:

$$R(x) = (\text{Docking Score}(x)^5 \times \text{QED}(x))^{\frac{1}{6}} \in [0, 1] \quad (1)$$

55 where x is a generated SMILES and the exponential terms apply more weighting to docking, i.e.,
 56 its contribution to the reward is greater than QED score⁴⁶ which is an empirical measure of "drug-
 57 likeness" (see Appendix C for more details). All experiments were run across 10 seeds (0-9 inclusive)
 58 with 3,000 oracle calls.

59 **Ultra-large Make-on-demand Library.** WuXi GalaXi⁴⁷ contains billions of make-on-demand
 60 molecules and the sheer size makes screening (even with active learning^{48,49}) computationally
 61 expensive. We consider two pseudo-randomly constructed subsets which we call WuXi (84,243,879)
 62 and WuXi-Large (756,642,169). See Appendix B for details. Extracted substructures from DBE are
 63 used to find match WuXi compounds that contain the substructure. The rationale for considering
 64 subsets differing by an order of magnitude is to increase the chances of a sufficient number of matches
 65 (1,000 in this work), as *large* substructures are necessarily specific.

66 **Experimental Setup.** Augmented Memory was tasked to generate molecules satisfying the objective
 67 function (Eq. 1) across 10 replicates (10 seeds, 0-9 inclusive). DBE was run on all 10 model
 68 checkpoints, extracting substructures with either a minimum token length of 20 or 25. These
 69 substructures were then used to find 1,000 matching compounds in the WuXi subsets, which were
 70 then assessed according to the same objective function (Eq. 1) and compared to random sampling.
 71 We note that experiments that did not match 1,000 compounds could be rescued by screening a larger
 72 WuXi subset, as WuXi-Large, despite containing >700M molecules, is a small fraction of WuXi
 73 GalaXi.

74 3 Results and Discussion

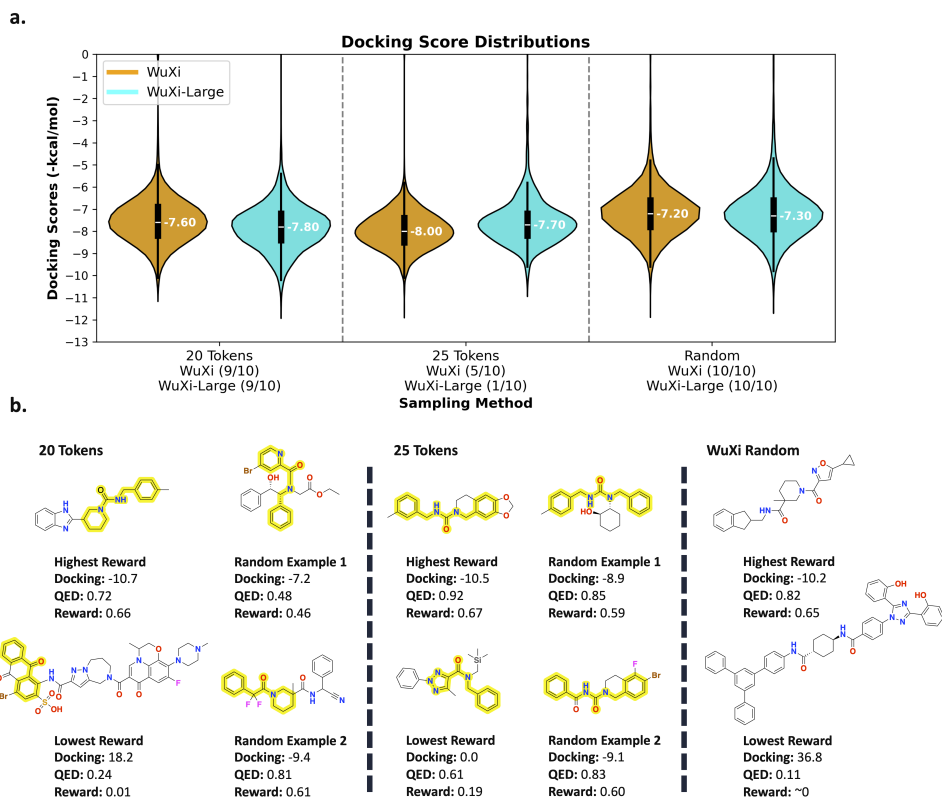


Figure 2: Docking scores distribution and example extracted substructures. **a.** Docking scores distribution of matched compounds vs. random sampling across WuXi and Wuxi-Large. **b.** Example extracted substructures using Dynamic Beam Enumeration and also showing the best and worst (by reward) and randomly matched compounds.

75 **Quantitative Results.** Fig. 2a shows the distribution of pooled (all runs that successfully matched
 76 1,000 compounds) docking scores comparing DBE-matched compounds vs. random sampling. The
 77 docking scores of the matched compounds possess better docking scores, on average, than random
 78 sampling (statistically significant). For plots of QED and reward, see Appendix D. Next, Table
 79 1 shows the mean and standard deviation of all properties. Note that reward is the aggregated
 80 "goodness" of a molecule, calculated based on Eq. 1. We make the following observations: firstly,
 81 on the WuXi subset, DBE outperforms random sampling and extracting *larger* substructures (25
 82 vs. 20) further improves property values. Secondly, *both* docking scores and QED are improved
 83 because both properties are part of the objective function (Eq. 1). Thirdly, matched compounds
 84 maintain diversity which is often desirable in screening campaigns (Table 2). However, we note that
 85 this improvement is inconsistent as matching compounds on the WuXi-Large subset can result in
 86 worse QED. For future work, it would be straightforward to add additional physico-chemical property
 87 checks to guard against this by discarding matched molecules with poor QED, since it is cheap to
 88 compute. We further note that the reason for inconsistent results between WuXi and WuXi-Large
 89 may be due to the significantly decreased diversity of WuXi-Large (Table 2). Consequently, matched
 90 compounds may be *too* similar, rather than being a set of more distinctive compounds that simply
 91 share common substructures. The straightforward solution is to further increase the subset size and
 92 diversity. This would also increase the chances of matching 1,000 compounds.

93 **Qualitative Results.** Fig. 2b shows the best and worst (by reward) and two random examples
 94 of matched compounds. We make the following observations: firstly, the best randomly sampled
 95 molecule is comparable to the best DBE molecules, but on average, they are worse (Table 1). Secondly,
 96 the substructures extracted from different model checkpoints via DBE can converge, as evidenced
 97 by identical substructures highlighted (Fig. 2) Thirdly, molecules with poor docking scores can be
 98 particularly large or contain undesirable atoms, e.g., Si, and it would be straightforward for future
 99 work to add a filter for these when matching. Moreover, it is well known that docking scores can
 100 be artificially inflated for molecules with high molecular weight and logP⁵⁰. Consequently, we
 101 analyzed select physico-chemical property distributions of the DBE matched vs. randomly sampled
 102 compounds (Fig. D5). Interestingly, DBE-matched compounds may not only possess better docking
 103 and QED values, but can also be smaller with less heavy atoms and polar surface area. This supports
 104 the efficacy of our workflow and shows promise for future development. Finally, the results show that
 105 information extracted from a generative model can be made *actionable* and that the substructures
 106 themselves are chemically meaningful, otherwise, such heavily biased matching would not result in a
 107 statistically significant improvement over random sampling.

Table 1: Extracted substructures are used to find compounds with the matching substructure in the WuXi datasets. The numbers in parenthesis denote the number of replicates out of 10 that were successful in matching 1,000 compounds. All compounds were pooled and the mean and standard deviation for docking, QED, and reward are reported.

Method	WuXi (84,243,879)			WuXi-Large (756,642,169)		
	Docking	QED	Reward	Docking	QED	Reward
Random (10, 10)	-7.13 ± 1.23	0.55 ± 0.19	0.47 ± 0.06	-7.17 ± 1.29	0.50 ± 0.16	0.46 ± 0.06
Dynamic Beam Enumeration						
20 Tokens (9, 9)	-7.52 ± 1.15	0.60 ± 0.22	0.49 ± 0.06	-7.82 ± 1.04	0.41 ± 0.15	0.47 ± 0.05
25 Tokens (5, 1)	-7.96 ± 0.83	0.74 ± 0.16	0.53 ± 0.04	-7.56 ± 1.08	0.36 ± 0.15	0.45 ± 0.05

108 4 Conclusion

109 In this work, we introduced **Dynamic Beam Enumeration (DBE)** as an extension to Beam Enumer-
 110 ation³⁸. By extracting *larger* substructures from a generative model checkpoint, they can be used to
 111 find matching compounds in ultra-large make-on-demand datasets. Our results show that matched
 112 compounds have properties more aligned with the desired property profile than random sampling
 113 (Table 1), while maintaining diversity (Table 2). Future work will investigate different beam pruning
 114 methods, add filtering checks to discard matched compounds with poor physico-chemical properties,
 115 and extract larger substructures (>25 tokens). Our method demonstrates the potential for DBE to
 116 act as a bridge between generative design and library screening, showing how extracted chemical
 117 insights can be made *actionable*.

References

1. Yuanqi Du, Arian R Jamasb, Jeff Guo, Tianfan Fu, Charles Harris, Yingheng Wang, Chenru Duan, Pietro Liò, Philippe Schwaller, and Tom L Blundell. Machine learning-aided generative molecular design. *Nature Machine Intelligence*, pages 1–16, 2024.
2. Julius Seumer, Jonathan Kirschner Solberg Hansen, Mogens Brøndsted Nielsen, and Jan H Jensen. Computational evolution of new catalysts for the morita–baylis–hillman reaction. *Angewandte Chemie International Edition*, 62(18):e202218565, 2023.
3. Peter Ertl and Ansgar Schuffenhauer. Estimation of synthetic accessibility score of drug-like molecules based on molecular complexity and fragment contributions. *Journal of cheminformatics*, 1:1–11, 2009.
4. Shuan Chen and Yousung Jung. Estimating the synthetic accessibility of molecules with building block and reaction-aware sascore. *Journal of Cheminformatics*, 2024.
5. Milan Voršilák, Michal Kolář, Ivan Čmelo, and Daniel Svozil. Syba: Bayesian estimation of synthetic accessibility of organic compounds. *Journal of cheminformatics*, 12:1–13, 2020.
6. Connor W Coley, Luke Rogers, William H Green, and Klavs F Jensen. Scscore: synthetic complexity learned from a reaction corpus. *Journal of chemical information and modeling*, 58(2):252–261, 2018.
7. John Bradshaw, Brooks Paige, Matt J Kusner, Marwin Segler, and José Miguel Hernández-Lobato. A model to search for synthesizable molecules. *Advances in Neural Information Processing Systems*, 32, 2019.
8. John Bradshaw, Brooks Paige, Matt J Kusner, Marwin Segler, and José Miguel Hernández-Lobato. Barking up the right tree: an approach to search over molecule synthesis dags. *Advances in neural information processing systems*, 33:6852–6866, 2020.
9. Ksenia Korovina, Sailun Xu, Kirthevasan Kandasamy, Willie Neiswanger, Barnabas Poczos, Jeff Schneider, and Eric Xing. Chembo: Bayesian optimization of small organic molecules with synthesizable recommendations. In *International Conference on Artificial Intelligence and Statistics*, pages 3393–3403. PMLR, 2020.
10. Sai Krishna Gottipati, Boris Sattarov, Sufeng Niu, Yashaswi Pathak, Haoran Wei, Shengchao Liu, Simon Blackburn, Karam Thomas, Connor Coley, Jian Tang, et al. Learning to navigate the synthetically accessible chemical space using reinforcement learning. In *International conference on machine learning*, pages 3668–3679. PMLR, 2020.
11. Julien Horwood and Emmanuel Noutahi. Molecular design in synthetically accessible chemical space via deep reinforcement learning. *ACS omega*, 5(51):32984–32994, 2020.
12. Wenhao Gao, Rocío Mercado, and Connor W Coley. Amortized tree generation for bottom-up synthesis planning and synthesizable molecular design. *Proc. 10th International Conference on Learning Representations*, 2022.
13. Kyle Swanson, Gary Liu, Denise B Catacutan, Autumn Arnold, James Zou, and Jonathan M Stokes. Generative ai for designing and validating easily synthesizable and structurally novel antibiotics. *Nature Machine Intelligence*, 6(3):338–353, 2024.
14. Miruna Cretu, Charles Harris, Julien Roy, Emmanuel Bengio, and Pietro Liò. Synflownet: Towards molecule design with guaranteed synthesis pathways. *arXiv preprint arXiv:2405.01155*, 2024.
15. Michał Koziarski, Andrei Rekish, Dmytro Shevchuk, Almer van der Sloot, Piotr Gaiński, Yoshua Bengio, Cheng-Hao Liu, Mike Tyers, and Robert A Batey. Rgfn: Synthesizable molecular generation using gflownets. *arXiv preprint arXiv:2406.08506*, 2024.
16. Marwin HS Segler and Mark P Waller. Neural-symbolic machine learning for retrosynthesis and reaction prediction. *Chemistry—A European Journal*, 23(25):5966–5971, 2017.

- 165 17. Marwin HS Segler, Mike Preuss, and Mark P Waller. Planning chemical syntheses with deep
166 neural networks and symbolic ai. *Nature*, 555(7698):604–610, 2018.
- 167 18. Krzysztof Maziarz, Austin Tripp, Guoqing Liu, Megan Stanley, Shufang Xie, Piotr Gaiński,
168 Philipp Seidl, and Marwin Segler. Re-evaluating retrosynthesis algorithms with syntheseus.
169 *arXiv preprint arXiv:2310.19796*, 2023.
- 170 19. Samuel Genheden, Amol Thakkar, Veronika Chadimová, Jean-Louis Reymond, Ola Engkvist,
171 and Esben Bjerrum. Aizynthfinder: a fast, robust and flexible open-source software for retrosyn-
172 thetic planning. *Journal of cheminformatics*, 12(1):70, 2020.
- 173 20. Lakshidaa Saigiridharan, Alan Kai Hassen, Helen Lai, Paula Torren-Peraire, Ola Engkvist, and
174 Samuel Genheden. Aizynthfinder 4.0: developments based on learnings from 3 years of industrial
175 application. *Journal of Cheminformatics*, 16(1):57, 2024.
- 176 21. Ian A Watson, Jibo Wang, and Christos A Nicolaou. A retrosynthetic analysis algorithm
177 implementation. *Journal of cheminformatics*, 11:1–12, 2019.
- 178 22. Connor W Coley, Luke Rogers, William H Green, and Klavs F Jensen. Computer-assisted
179 retrosynthesis based on molecular similarity. *ACS central science*, 3(12):1237–1245, 2017.
- 180 23. Connor W Coley, Dale A Thomas III, Justin AM Lummiss, Jonathan N Jaworski, Christopher P
181 Breen, Victor Schultz, Travis Hart, Joshua S Fishman, Luke Rogers, Hanyu Gao, et al. A robotic
182 platform for flow synthesis of organic compounds informed by ai planning. *Science*, 365(6453):
183 eaax1566, 2019.
- 184 24. Philippe Schwaller, Riccardo Petraglia, Valerio Zullo, Vishnu H Nair, Rico Andreas Haeuselmann,
185 Riccardo Pisoni, Costas Bekas, Anna Iuliano, and Teodoro Laino. Predicting retrosynthetic
186 pathways using transformer-based models and a hyper-graph exploration strategy. *Chemical
187 science*, 11(12):3316–3325, 2020.
- 188 25. Amol Thakkar, Alain C Vaucher, Andrea Byekwaso, Philippe Schwaller, Alessandra Toniato,
189 and Teodoro Laino. Unbiasing retrosynthesis language models with disconnection prompts. *ACS
190 Central Science*, 9(7):1488–1498, 2023.
- 191 26. IBM. Rxn for chemistry.
- 192 27. Sara Szymkuć, Ewa P Gajewska, Tomasz Klucznik, Karol Molga, Piotr Dittwald, Michał Startek,
193 Michał Bajczyk, and Bartosz A Grzybowski. Computer-assisted synthetic planning: the end of
194 the beginning. *Angewandte Chemie International Edition*, 55(20):5904–5937, 2016.
- 195 28. Bartosz A Grzybowski, Sara Szymkuć, Ewa P Gajewska, Karol Molga, Piotr Dittwald, Agnieszka
196 Wołos, and Tomasz Klucznik. Chematica: a story of computer code that started to think like a
197 chemist. *Chem*, 4(3):390–398, 2018.
- 198 29. Jeff Guo and Philippe Schwaller. Saturn: Sample-efficient generative molecular design using
199 memory manipulation. *arXiv preprint arXiv:2405.17066*, 2024.
- 200 30. Jeff Guo and Philippe Schwaller. Directly optimizing for synthesizability in generative molecular
201 design using retrosynthesis models. *arXiv preprint arXiv:2407.12186*, 2024.
- 202 31. Jason D Shields, Rachel Howells, Gillian Lamont, Yin Leilei, Andrew Madin, Christopher E
203 Reimann, Hadi Rezaei, Tristan Reuillon, Bryony Smith, Clare Thomson, et al. Aizynth impact
204 on medicinal chemistry practice at astrazeneca. *RSC Medicinal Chemistry*, 15(4):1085–1095,
205 2024.
- 206 32. Jiankun Lyu, Sheng Wang, Trent E Balius, Isha Singh, Anat Levit, Yurii S Moroz, Matthew J
207 O’Meara, Tao Che, Enkhjargal Alгаа, Kateryna Tolmachova, et al. Ultra-large library docking
208 for discovering new chemotypes. *Nature*, 566(7743):224–229, 2019.
- 209 33. Christoph Gorgulla, Andras Boeszoermyenyi, Zi-Fu Wang, Patrick D Fischer, Paul W Coote,
210 Krishna M Padmanabha Das, Yehor S Malets, Dmytro S Radchenko, Yurii S Moroz, David A
211 Scott, et al. An open-source drug discovery platform enables ultra-large virtual screens. *Nature*,
212 580(7805):663–668, 2020.

- 213 34. Christoph Gorgulla, AkshatKumar Nigam, Matt Koop, Süleyman Selim Çınaroğlu, Christopher
214 Secker, Mohammad Haddadnia, Abhishek Kumar, Yehor Malets, Alexander Hasson, Minkai Li,
215 et al. Virtualflow 2.0-the next generation drug discovery platform enabling adaptive screens of
216 69 billion molecules. *bioRxiv*, pages 2023–04, 2023.
- 217 35. Arman A Sadybekov, Anastasiia V Sadybekov, Yongfeng Liu, Christos Iliopoulos-Tsoutsouvas,
218 Xi-Ping Huang, Julie Pickett, Blake Houser, Nilkanth Patel, Ngan K Tran, Fei Tong, et al.
219 Synthon-based ligand discovery in virtual libraries of over 11 billion compounds. *Nature*, 601
220 (7893):452–459, 2022.
- 221 36. François Sindt, Anthony Seyller, Merveille Eguida, and Didier Rognan. Protein structure-based
222 organic chemistry-driven ligand design from ultralarge chemical spaces. *ACS Central Science*,
223 10(3):615–627, 2024.
- 224 37. Fangyu Liu, Olivier Mailhot, Isabella S Glenn, Seth F Vigneron, Viola Bassim, Xinyu Xu, Karla
225 Fonseca-Valencia, Matthew S Smith, Dmytro S Radchenko, James S Fraser, et al. The impact of
226 library size and scale of testing on virtual screening. *bioRxiv*, pages 2024–07, 2024.
- 227 38. Jeff Guo and Philippe Schwaller. Beam enumeration: Probabilistic explainability for sample
228 efficient self-conditioned molecular design. In *Proc. 12th International Conference on Learning*
229 *Representations*, 2024.
- 230 39. Jeff Guo and Philippe Schwaller. Augmented memory: Sample-efficient generative molecular
231 design with reinforcement learning. *JACS Au*, 2024.
- 232 40. Sepp Hochreiter and Jürgen Schmidhuber. Long short-term memory. *Neural computation*, 9(8):
233 1735–1780, 1997.
- 234 41. David Weininger. Smiles, a chemical language and information system. 1. introduction to
235 methodology and encoding rules. *Journal of chemical information and computer sciences*, 28(1):
236 31–36, 1988.
- 237 42. Oleg Trott and Arthur J Olson. Autodock vina: improving the speed and accuracy of docking
238 with a new scoring function, efficient optimization, and multithreading. *Journal of computational*
239 *chemistry*, 31(2):455–461, 2010.
- 240 43. Amr Alhossary, Stephanus Daniel Handoko, Yuguang Mu, and Chee-Keong Kwoh. Fast, accurate,
241 and reliable molecular docking with quickvina 2. *Bioinformatics*, 31(13):2214–2216, 2015.
- 242 44. Shidi Tang, Ji Ding, Xiangyu Zhu, Zheng Wang, Haitao Zhao, and Jiansheng Wu. Vina-gpu
243 2.1: towards further optimizing docking speed and precision of autodock vina and its derivatives.
244 *bioRxiv*, pages 2023–11, 2023.
- 245 45. Mark F Mabanglo, Keith S Wong, Marim M Barghash, Elisa Leung, Stephanie HW Chuang,
246 Afshan Ardalani, Emily M Majaesic, Cassandra J Wong, Shen Zhang, Henk Lang, et al. Potent
247 clpp agonists with anticancer properties bind with improved structural complementarity and alter
248 the mitochondrial n-terminome. *Structure*, 31(2):185–200, 2023.
- 249 46. G Richard Bickerton, Gaia V Paolini, Jérémy Besnard, Sorel Muresan, and Andrew L Hopkins.
250 Quantifying the chemical beauty of drugs. *Nature chemistry*, 4(2):90–98, 2012.
- 251 47. WuXi. Virtual screening. URL [https://wuxibiology.com/drug-discovery-services/
252 hit-finding-and-screening-services/virtual-screening/](https://wuxibiology.com/drug-discovery-services/hit-finding-and-screening-services/virtual-screening/).
- 253 48. Antonio Lavecchia and Carmen Di Giovanni. Virtual screening strategies in drug discovery: a
254 critical review. *Current medicinal chemistry*, 20(23):2839–2860, 2013.
- 255 49. David E Graff, Eugene I Shakhnovich, and Connor W Coley. Accelerating high-throughput
256 virtual screening through molecular pool-based active learning. *Chemical science*, 12(22):
257 7866–7881, 2021.
- 258 50. John A Arnott and Sonia Lobo Planey. The influence of lipophilicity in drug discovery and
259 design. *Expert opinion on drug discovery*, 7(10):863–875, 2012.

- 260 51. Rdkit: Open-source cheminformatics. URL <http://www.rdkit.org>.
- 261 52. Daniil Polykovskiy, Alexander Zhebrak, Benjamin Sanchez-Lengeling, Sergey Golovanov, Oktai
262 Tatanov, Stanislav Belyaev, Rauf Kurbanov, Aleksey Artamonov, Vladimir Aladinskiy, Mark
263 Veselov, et al. Molecular sets (moses): a benchmarking platform for molecular generation models.
264 *Frontiers in pharmacology*, 11:565644, 2020.
- 265 53. Yutong Xie, Ziqiao Xu, Jiaqi Ma, and Qiaozhu Mei. How much space has been explored?
266 measuring the chemical space covered by databases and machine-generated molecules. In *Proc.*
267 *11th International Conference on Learning Representations*, 2023.

268 Appendix

269 The Appendix contains details on how Dynamic Beam Enumeration extracts substructures, the WuXi
270 GalaXi⁴⁷ make-on-demand library, reward shaping details, and additional results.

271 A Dynamic Beam Enumeration: How are Substructures Extracted?

272 In this section, we discuss more in detail the formulation of the original Beam Enumeration³⁸, how
273 Dynamic Beam Enumeration extends the method, and finally, how substructures are extracted from
274 token sequences. Beam Enumeration exhaustively enumerates the top k highest probability tokens
275 from autoregressive language-based molecular generative models. When $k = 2$, this results in 2^N
276 sub-sequences, where N (18 in this work) is the number of beam steps. As the generative model
277 is autoregressive, every sub-sequence has an associated probability given by the product of the
278 individual token probabilities. For example, the sub-sequence "CN" has a probability of $P(C) * P(N |$
279 $C)$. Dynamic Beam Enumeration stores these probabilities for all enumerated sub-sequences, sorts
280 them, then prunes the set and keeps only the highest 2^{N-M} subsequences. M is 12 in this work,
281 therefore $2^6 = 64$ were kept. Next, these 64 sub-sequences were further enumerated for 12 steps,
282 resulting in token sub-sequences of length $M + N$ tokens = 30. Substructures are then extracted
283 exactly as formulated in the original Beam Enumeration work: every consecutive sub-sub-sequence
284 is considered and those that map to valid RDKit⁵¹ molecules are stored. For example, consider the
285 sub-sequence ABCDEF. The set of consecutive sub-sub-sequences are A, AB, ABC, ABCD, ABCDE,
286 ABCDEF. Every single sub-sequence undergoes this process and the substructure frequencies are
287 summed up. The top-4 most frequently appearing substructures are the set of extracted substructures.
288 Finally, Dynamic Beam Enumeration enforces the minimum token length of the substructures to be
289 either 20 or 25 in this work. This ensures that the substructures are *larger* than the original Beam
290 Enumeration work which only considered substructures with minimum token length as long as 15.

291 B WuXi GalaXi: Ultra-large Make-on-demand Library

292 WuXi GalaXi⁴⁷ contains billions of make-on-demand molecules. Dynamic Beam Enumeration
293 extracted substructures are used to *match* compounds with these corresponding substructures. As
294 searching through such a large database can be computationally prohibitive, we create two smaller
295 sub-sets of WuXi in a pseudo-random manner. In this section, we detail the construction process
296 of the two datasets which we call **WuXi** and **WuXi-Large**. Note that WuXi GalaXi is provided in
297 **Phases** which can contain multiple **Parts**, each composed of a set of SMILES. Construction of the
298 datasets involved extracting the raw zip files from WuXi GalaXi. Due to the size of the files, we
299 performed the extraction for an arbitrary amount of time (not extracting the full file). This is why
300 every file extraction as described below contains a seemingly completely random number of SMILES.

301 B.1 WuXi

302 **WuXi** was constructed by taking the entire **Phase 1** (24,093,421 SMILES) and part of **Phase 2 Part 3**
303 (the first 60,150,458 SMILES). This was done arbitrarily and resulted in **84,243,879 total SMILES**.

304 B.2 WuXi-Large

305 **WuXi-Large** was constructed by taking some SMILES from all six parts of **WuXi Phase 2**.

- 306 • Part 1: First 125,821,918
- 307 • Part 2: First 122,345,617
- 308 • Part 3: First 133,357,788
- 309 • Part 4: First 132,610,455
- 310 • Part 5: First 120,735,841
- 311 • Part 6: First 121,770,550

312 This was done arbitrarily and resulted in **756,642,169 total SMILES**.

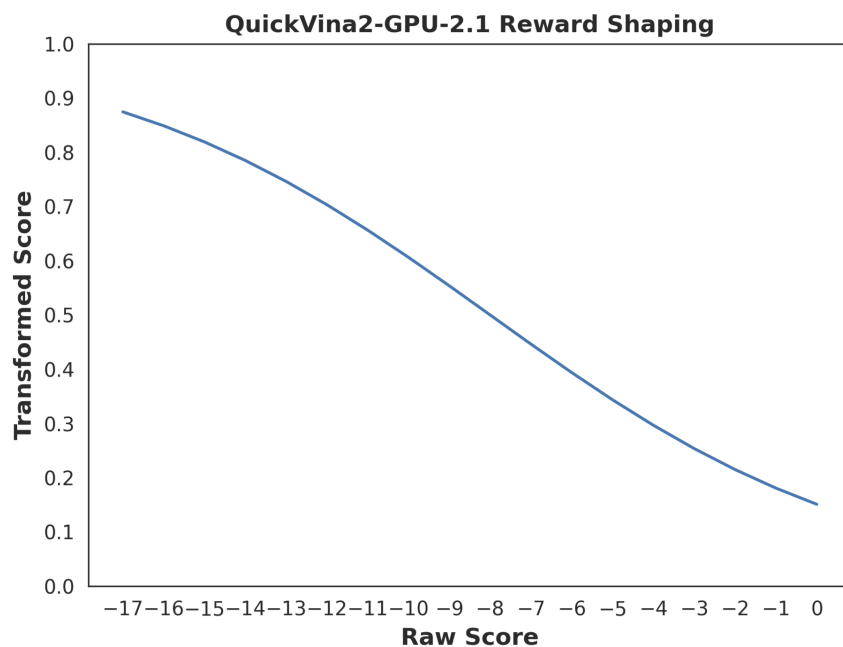


Figure C3: Reward shaping function for QuickVina2-GPU-2.1.

313 C Reward Shaping

314 This section contains details on the reward shaping functions used during Augmented Memory³⁹
 315 goal-directed generation. Fig. C3 shows the function for QuickVina2-GPU-2.1⁴²⁻⁴⁴ docking scores.
 316 For QED⁴⁶, raw values were used. Subsequently, the reward-shaped docking scores and raw QED
 317 values were aggregated to a single scalar following the equation below:

$$R(x) = \left[\prod_i p_i(x)^{w_i} \right]^{\frac{1}{\sum_i w_i}} \quad (2)$$

318 where x is a SMILES⁴¹, i is the index of an oracle given many oracles (MPO objective), p_i is an oracle,
 319 and w_i is the weight assigned to the oracle. In this work, the oracles were QuickVina2-GPU-2.1⁴²⁻⁴⁴
 320 docking and QED⁴⁶ with weights of 5 and 1, respectively.

321 D Additional Results

322 This section contains supplementary plots comparing Dynamic Beam Enumeration matched com-
 323 pounds vs. random sampling in WuXi and WuXi-Large. Fig. D4 shows the distributions of docking
 324 scores, QED, and reward. Fig. D5 shows the distributions of molecular weight, topological polar
 325 surface area (tPSA), and number of heavy atoms. Table 2 contains statistics on the internal diversity
 326 (IntDiv1)⁵² and #Circles⁵³ with threshold = 0.75 of the matched vs. randomly sampled compounds.
 327 We note that WuXi-Large is notably less diverse than the smaller WuXi.

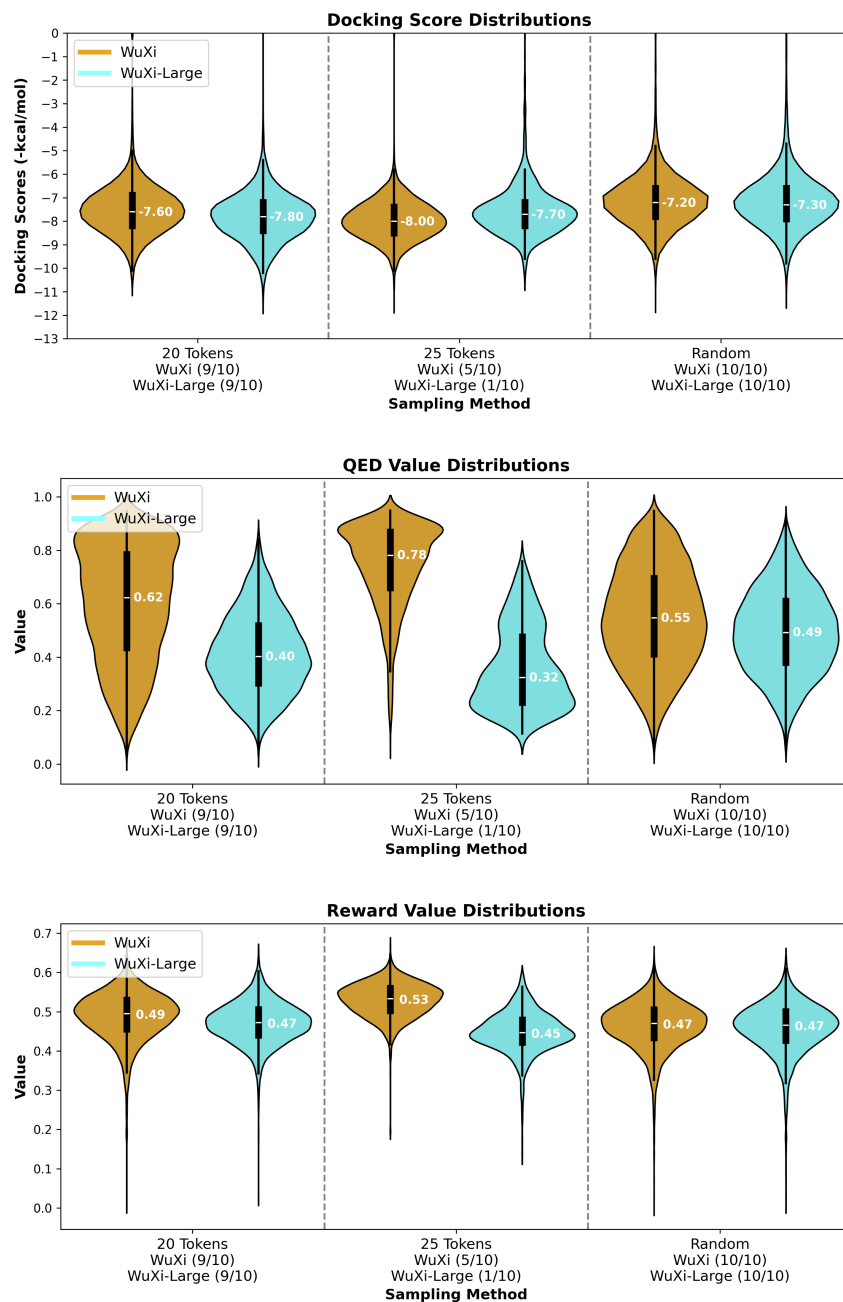


Figure D4: Distributions of oracle values.

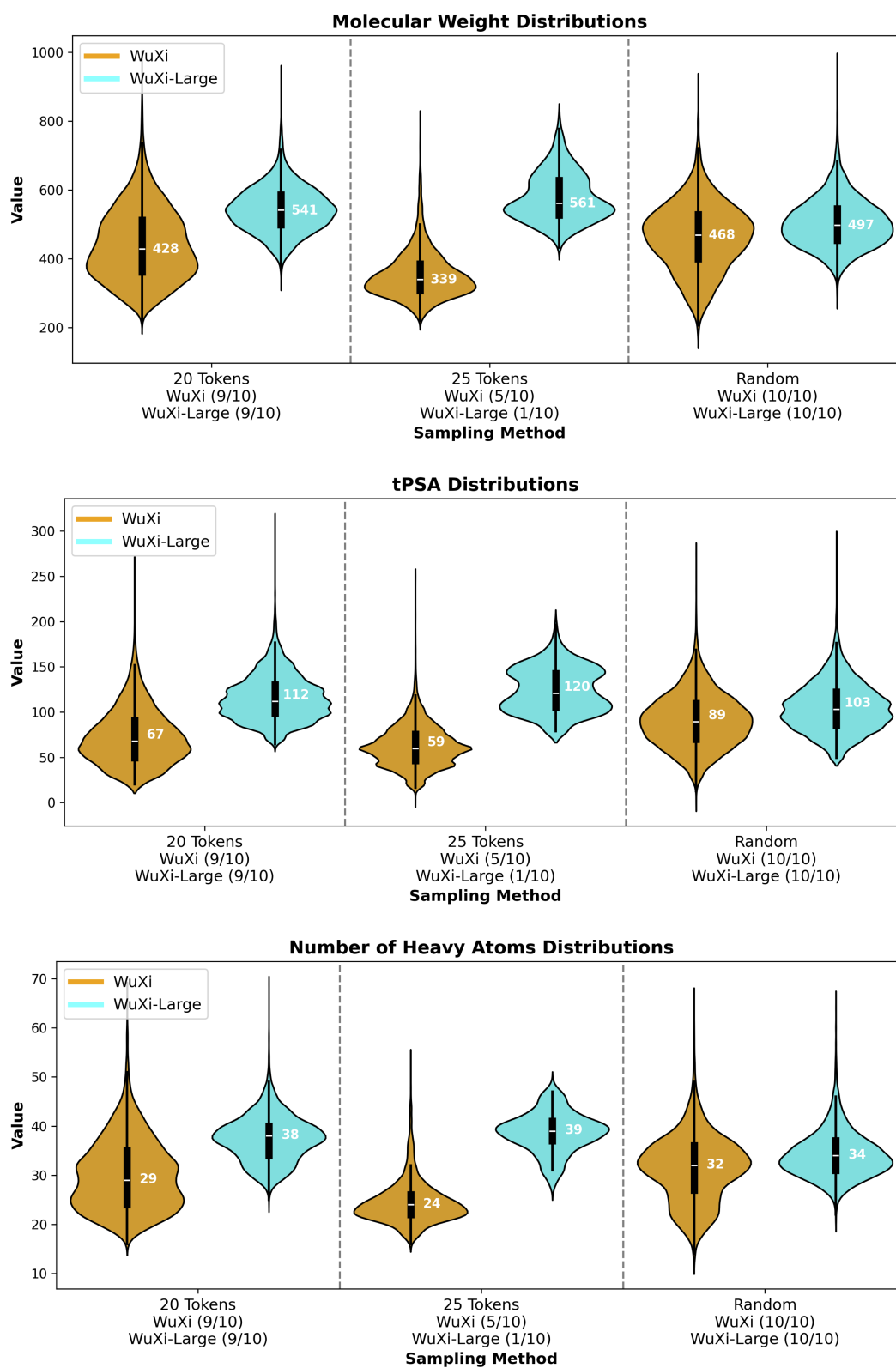


Figure D5: Distributions of property values.

Table 2: Diversity of WuXi matched compounds vs. randomly sampled. The numbers in parenthesis denote the number of replicates out of 10 that were successful in matching 1,000 compounds. All compounds were pooled and the mean and standard deviation for IntDiv1 and #Circles are reported.

Method	WuXi (84,243,879)		WuXi-Large (756,642,169)	
	IntDiv1	#Circles (Threshold = 0.75)	IntDiv1	#Circles (Threshold = 0.75)
Random (10, 10)	0.826 \pm 0.001	90 \pm 0.7	0.773 \pm 0.002	5 \pm 1
Dynamic Beam Enumeration				
20 Tokens (9, 9)	0.781 \pm 0.035	20 \pm 10	0.630 \pm 0.039	1 \pm 1
25 Tokens (5, 1)	0.743 \pm 0.027	8 \pm 3	0.741 \pm 0.000	4 \pm 0